ANTICANCER RESEARCH *41*: 5249-5254 (2021)
doi:10.21873/anticanres.15344

Intrahepatic Cholangiocarcinoma Coexisting With Multiple Bile Duct Adenoma Treated as Liver Metastasis from a Pancreatic Neuroendocrine Tumor

ERI ODA[1], KENSUKE YAMAMURA[1], YOSHIHIRO HARA[1], KAZUKI MATSUMURA[1], SHINICHI AKAHOSHI[1], HIDEAKI YUKI[2], TOSHIHIKO MOTOHARA[3], HIDEAKI MIYAMOTO[4], KOICHI KINOSHITA[5], FUJIO MATSUMURA[5], KOJI OHNISHI[6], YOSHIHIRO KOMOHARA[7] and TORU BEPPU[1]

[1]*Department of Surgery, Yamaga City Medical Center, Kumamoto, Japan;*
[2]*Department of Radiology, Yamaga City Medical Center, Kumamoto, Japan;*
[3]*Department of Gastroenterology, Yamaga City Medical Center, Kumamoto, Japan;*
[4]*Department of Medical Oncology, Yamaga City Medical Center, Kumamoto, Japan;*
[5]*Department of Surgery, Tenryo Hospital, Fukuoka, Japan;*
[6]*Department of Community Network Pathology, Kumamoto University Hospital, Kumamoto, Japan;*
[7]*Department of Cell Pathology, Graduate School of Medicine, Kumamoto University, Kumamoto, Japan*

Abstract. *Background: Bile duct adenomas (BDA) may be precursor lesions of small duct-type, including mass-forming type intrahepatic cholangiocarcinoma (ICC). Case Report: A 68-year-old woman was transferred to our facility for the treatment of a liver tumor, possibly metastasized from a pancreatic neuroendocrine tumor. Finally, two liver tumors were resected and histopathologically diagnosed as "BDA" and "ICC with a BDA-like component". In the BDA-like component, the MUC6 positive rate was notably lower and the Ki-67 positive rate was higher than the other BDAs and ICC component, respectively. The doubling time of the tumor volume in BDA was very long but was shortened (1,510 and 719 days). Distinct enlargement of the tumor and appearance of enhancement through diagnostic imaging was useful in diagnosing the transformation from a BDA to an ICC. Conclusion: An "adenoma-carcinoma sequence" may exist in the transformation process from a BDA to an ICC.*

Pancreatic neuroendocrine tumors (pNET) are rare with an annual incidence of less than one case per 100,000 individuals; however, the rate of occurrence of the disease is increasing worldwide (1). The prognosis of a pNET depends on clinicopathological factors, including tumor size, proliferative index, and differentiation (2, 3). Surgical resection of the tumor is the only way to accomplish a cure for primary and metastatic pNETs. In patients with pNETs, the liver is the most common site of metastasis, with a frequency of approximately 28%-77% (4). Everolimus is a targeted drug that can improve progression-free survival in patients with advanced pNET and can cause interstitial pneumonia as a rare but severe adverse event (5). Liver metastases caused from pNET are known as hypervascular tumors in the arterial phase, and half of them were observed to be hypovascular in the portal venous phase through diagnostic imaging (6).

Bile duct adenoma (BDA) is incidentally observed during surgery or autopsy as a subcapsular liver tumor, ranging from 1 to 20 mm in diameter (7). Histopathologically, BDA is an isolated intrahepatic lesion consisting of many small homogeneous ducts with benign cuboidal cells and a narrow lumen (8). The concept of precursor lesions of large duct-type intrahepatic cholangiocarcinoma (ICC) is similar to the general concept of "adenoma-carcinoma sequence" in gastrointestinal tract cancer; however, peripheral small duct-type ICC may have a different histologic phenotype, which is the non-mucinous type, and shows homology or transitions to hepatocellular carcinoma (8). Nakanuma *et al.* reported a new subtype of ICC with a predominant "ductal plate malformation" pattern (9). Recently, it has been published that BDAs may be precursor lesions of small duct-type ICC that included mass-forming ICC (10). The incidence of BDA was significantly correlated with advanced age and the presence of von Meyenburg complexes. In fact, transitional areas can exist from BDA to ICC in the same tumor (11).

Correspondence to: Toru Beppu, Department of Surgery, Yamaga City Medical Center, 511, Yamaga, Kumamoto, 861-0593, Japan. Tel: +81 968442185, Fax: +81 968442420, e-mail: tbeppu@yamaga-mc.jp

Key Words: Bile duct adenoma, intrahepatic cholangiocarcinoma, liver metastasis, pancreatic neuroendocrine tumor.

BDAs are incidentally detected through radiological imaging mainly in chronically diseased or cirrhotic livers and present as single subcapsular or superficial lesions of the liver without capsule formation along with being <2 cm in size (12, 13). In previous reports on diagnostic imaging, BDAs generally show arterial phase hyperenhancement and delayed or prolonged enhancement due to the fibrous stroma components in the tumors (12). In contrast, small mass-forming-type ICC (<3 cm) show arterial phase hyperenhancement with washout or peripheral rim sign in the portal to venous phase (12, 14).

Herein, we present a case with ICC and multiple metachronous BDAs successfully treated with hepatectomy. The patient previously underwent systemic medical therapy with Everolimus for liver metastasis caused from pNET. Based on detailed histopathological examination, we can clearly demonstrate the "adenoma-carcinoma sequence" in the peripheral small duct-type ICC.

Case Report

A 68-year-old female patient was transferred to our hospital for the treatment of a liver tumor. Two and a half years ago, she underwent subtotal stomach preserving pancreaticoduodenectomy for pNET and partial liver resection for an unknown liver tumor at the referral hospital. The pancreatic tumor, 1.5 cm in diameter, showed perceptible hypervascularity in the arterial phase with a continuous enhanced effect. In contrast, the liver tumor was an unclear hypovascular tumor. The postoperative histopathology findings showed pNET (gastrinoma, stage IA) and BDA. Preoperative level of serum gastrin before stimulation was 770 pg/ml (normal range < 200 pg/ml). One and a half years after the surgery, a hypervascular liver tumor that mimicked pNET was detected in segment 8 and was subsequently diagnosed as metachronous liver metastasis of pNET without tumor biopsy. Administration of Everolimus was started but was discontinued after 3 months due to interstitial pneumonia. She was referred to our hospital for the treatment of the gradually growing liver tumor. The etiology included both hepatitis B surface antigen (−) and hepatitis C (HCV) antibody (+); however, HCV ribonucleic acid was not detected. The Child-Pugh score was 6 points. She had a low serum albumin level of 3.26 g/dl (normal range=4.1-5.1 g/dl) and an elevated 15-minute indocyanine green retention rate of 27.0% (normal range ≤10%). Total bilirubin, transaminase and prothrombin activity, and platelet count levels were all within normal limits. As for tumor markers, serum levels of alpha-fetoprotein, carbohydrate antigen 19-9, and neuron-specific enolase were within normal limits. Carcinoembryonic antigen (CEA) levels were elevated at 12.8 ng/ml (normal range ≤5 ng/ml) but also elevated at 14.5 ng/ml before the first operation. Contrast-enhanced computed tomography showed an early deep-stained tumor with a diameter of 22 mm in segment 8, which showed the same degree of enhancement as the liver parenchyma in the late phase. Gadolinium dethoxybenzyl-diethylenetriamine pentaacetic acid-enhanced (EOB) magnetic resonance imaging (MRI) showed mild hyperintensity on T2-weighted imaging, a high signal on diffusion-weighted imaging, and a low signal on the hepatobiliary phase (Figure 1A-E). Based on the clinical course, preoperative diagnosis of this tumor was liver metastasis caused by pNET. The tumor in segment 3 was slightly enhanced in the arterial phase and showed prolonged enhancement (Figure 1F-J). Higher signal on diffusion-weighted imaging was shown in the former than that in the latter. The tumor was suspected to be BDA. Segmentectomy of segment 8 and partial resection of the segment 3 tumor was performed. Postoperative histopathological results revealed poorly-differentiated ICC for an S8 lesion and BDA for an S3 lesion.

Serial MRI images demonstrated that the S8 tumor was definitely enlarging, whereas the S3 tumor remained stable in size (Figure 2). The tumor diameters were measured via MRI in the axial hepatobiliary phase (slice thickness: 4 mm) by radiologists with 15 years of experience. The doubling time of the tumor volume (TVDT) was investigated according to the previous papers (15-17). DT was 198 and 194 days for the S8 tumor and 1,510 and 719 days for the S3 tumor during the first and second periods, respectively.

Results of the detailed histopathological examination and immunohistochemistry profiling are summarized in Figure 3 and Table I. BDA1 was a liver tumor that was removed during surgery for pNET. The tumor showed mild atypical cells that proliferated in a cord-like or tubular shape (Figure 3A). The Ki-67 positive rate was <1%, and the MUC6 positive rate was 100% (Figure 3B and C). BDA2 was a resected lesion in segment 3. The tumor also showed a cord-like or tubular proliferation pattern (Figure 3D), and the Ki-67 and MUC6 positive rates were similar to those of BDA1 (Figure 3E and F). A small amount of BDA-like component (approximately 5%), with weak atypia, was observed in the ICC lesion (Figure 3G). The Ki-67 positive rate was low; however, the MUC6 positive rate was evidently lower than that of BDA1 and BDA2 (Figure 3H and I). ICC showed a glandular, cribriform, and solid growth pattern, with a high degree of fibrosis and infiltration of inflammatory cells (Figure 3J). The Ki-67 positive rate was relatively high, whereas the MUC6 positive rate was extremely low (Figure 3K and L).

The patient was discharged on postoperative day 11 from our hospital and is doing well without any recurrence 9 months after the second operation.

Discussion

The patient was transferred to our hospital for a hepatectomy due to a strongly suspicious liver metastasis in segment 8 caused by pNET. Although the patient had already been

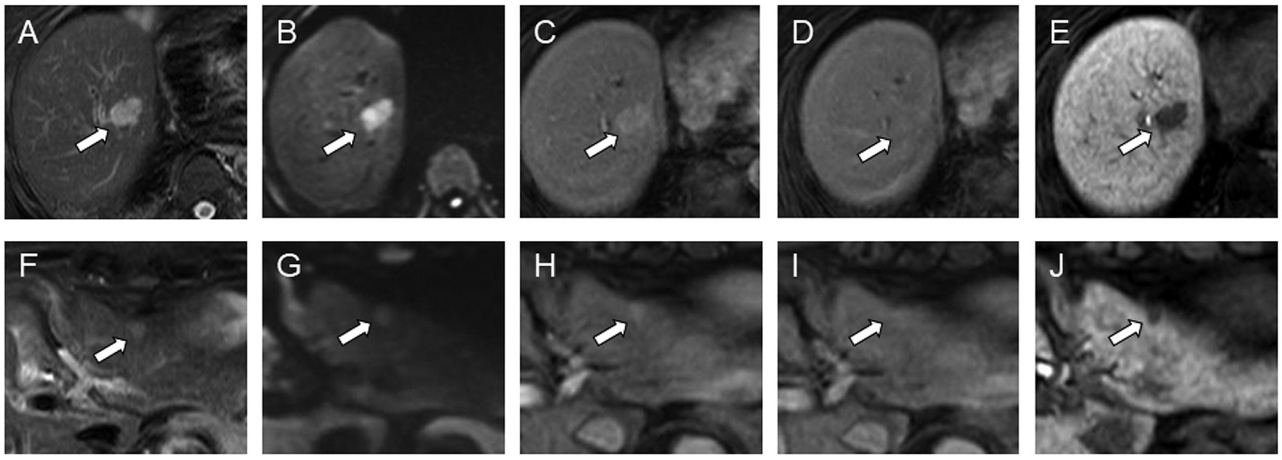

Figure 1. *Gadolinium dethoxybenzyl-diethylenetriamine pentaacetic acid-enhanced enhanced magnetic resonanse axial images of intrahepatic cholangiocarcinoma and bile duct adenoma. (A, F) Fat suppressed T2-weighted images; (B, G) Diffusion-weighted images; arterial phase (C, H), portal phase (D, I), and hepatobiliary phase (E, J) of the dynamic study images. Both tumors showed mild hyperintensity on T2-weighted images and high signal on diffusion-weighted images. The tumor showed early enhancement in arterial phases, mild delayed washout in portal phases, and low signal on hepato-biliary phases.*

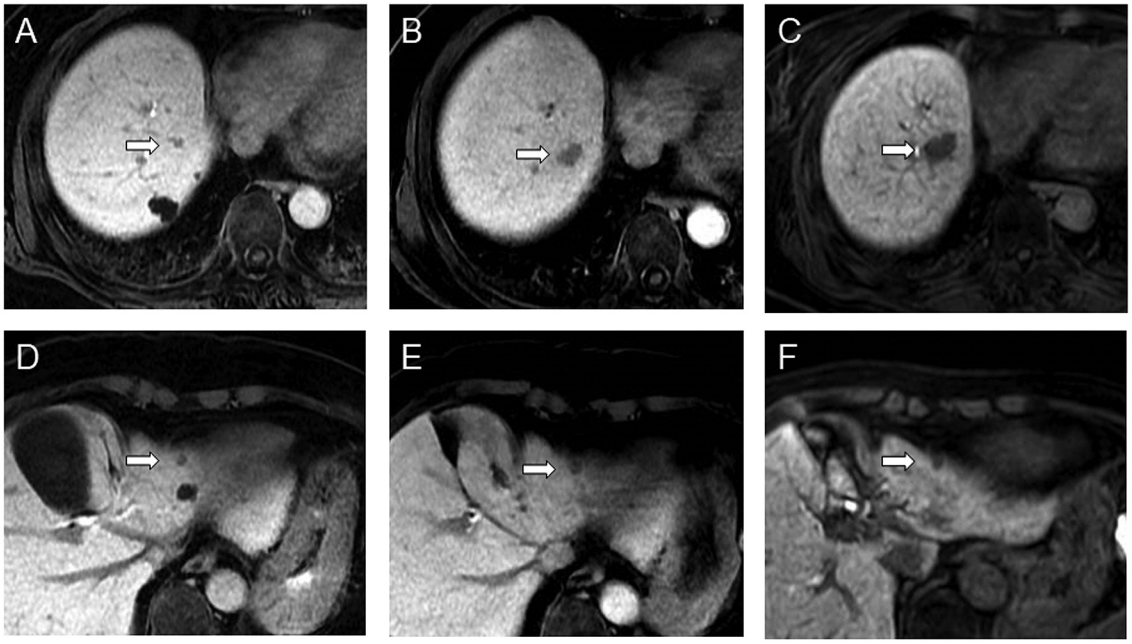

Figure 2. *Serial magnetic resonance imaging findings of intrahepatic cholangiocarcinoma and bile duct adenoma. The lesions (arrows) showed hypointensity on axial hepatobiliary phase at the pancreatic neuroendocrine tumor surgery (A and D), and at 22 months (B and E) and 34 months (C and F) after the surgery. Maximal diameters of the bile duct adenoma tumors were 8.4 mm, 9.3 mm, and 10.4 mm, and the intrahepatic cholangiocarcinoma tumors were 6.9 mm, 15.0 mm, and 22.7 mm.*

treated with Everolimus, the tumor showed progression. The primary pNET had been diagnosed as gastrinoma; however, serum gastrin levels were unfortunately not measured during the postoperative observation period. Although the tumor showed an enhancement pattern like that of liver metastasis from pNET by diagnostic imaging (6, 12), a tumor biopsy using a fine needle may be required before chemotherapy. However, percutaneous tumor biopsy or cytology is not

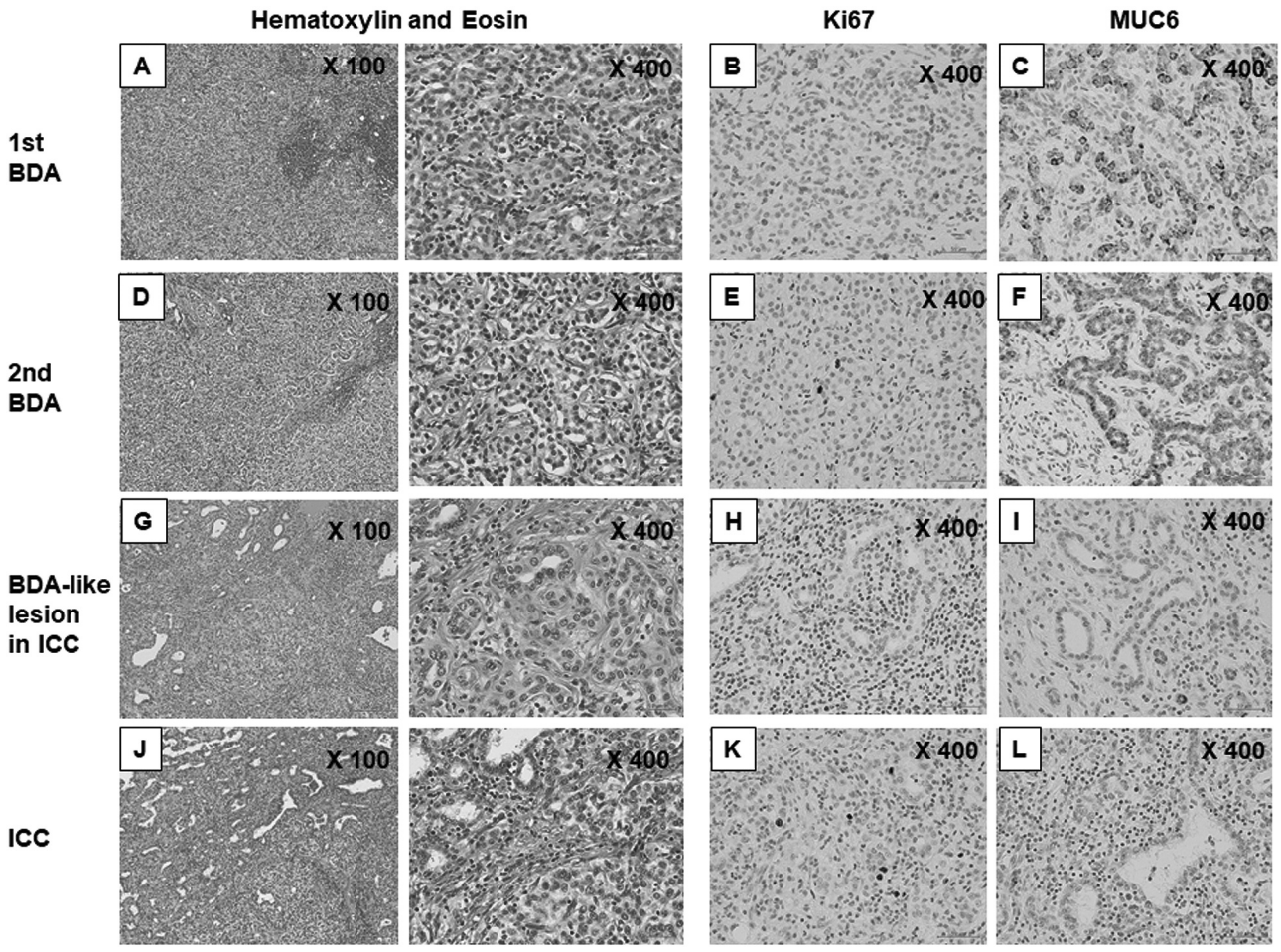

Figure 3. *Microscopic findings of the resected tumors. First line images: BDA1, the liver tumor at the time of initial surgery; 2nd line images: BDA2, the liver tumor in the segment 3 removed during the second surgery; 3rd line images: a bile duct adenoma-like component inside ICC; 4th Images: ICC resected during the second surgery. First and 2nd row images show hematoxylin-eosin staining and 3rd and 4th row images show immunohistochemical staining for Ki-67 and MUC-6. The magnification is shown in each slide. BDA: Bile duct adenoma; ICC: intrahepatic cholangiocarcinoma; MUC: mucin.*

recommended for highly malignant liver tumors, including ICC, because of increased risk of intraabdominal tumor seeding (18). Considering the implications of diagnostic treatment, a curative liver resection was performed.

At the time of pancreaticoduodenectomy, a small liver tumor was detected intraoperatively on the liver surface and was enucleated. The histopathological diagnosis was BDA. Fortunately, the other liver tumors in segments 8 and 3 could be followed-up through diagnostic imaging for 22 months. Finally, two tumors were resected, and the former was diagnosed as ICC, whereas the latter was diagnosed as BDA. In the previous papers, median TVDT of mass-forming ICC, HCC, and colorectal liver metastases (CRLM) was 70 days (range=14.5-512.9 days), 79.8 days (range=13.5-355.6 days), and 71.4 days (95% confidence interval=62.8-79.9), respectively (15-17). For our patient, all maximal tumor diameters were measured using the hepatobiliary images of EOB-MRI because of their clear tumor border. Actual TVDT was relatively long (198 and 194 days) for ICC and very long for BDA (1,510 and 719 days). Appearance of early enhancement was one of the signs of transformation from BDA to ICC (12). Upon reviewing the diagnostic images, the degree of early enhancement gradually increased in the tumor decisively diagnosed as ICC.

The ICC lesion contained less BDA-like tumor cells with low atypia (Figure 3G) in the patient. Furthermore, the BDA-like tumor component generally showed immunohistochemistry profiles similar to the IHC phenotype of BDA, in particular MUC6 and Ki67 (Figure 3H and 3I) (19). In a previous paper, it was demonstrated that the ICC lesion contained BDA-like

Table I. *Immunohistochemistry profile of four lesions*.

	BDA 1	BDA 2	BDA-like lesion in ICC	ICC
Ki67	<1%	1-2%	1-2%	2-5%
p53	<1%	1-2%	2-3%	2-3%
p16	80%	90%	40-50%	20-30%
CK19	100%	100%	90%	90%
MUC5AC	1%	40-50%	30-40%	30-40%
MUC6	100%	100%	30-40%	2-5%
CD68	10-20/HPF	30-50/HPF	60-100/HPF	60-100/HPF
CD163	5-10/HPF	30-60/HPF	80-150/HPF	80-150/HPF

BDA: Bile duct adenoma; ICC: intrahepatic cholangiocarcinoma; CK: cytokeratin; MUC: mucin; HPF: high power field.

components similar to our patient (11). Recent studies demonstrated that BDA is considered a true tumor with several genetic abnormalities, such as *BRAF* V600E mutation (20). Furthermore, if some genetic abnormalities of ARID1A, p53, or PBRM1 are added to a BDA, it may transform into small duct-type ICC (10). These findings suggest that the BDA may have transformed into ICC in our patient.

In conclusion, our patient may have demonstrated the "adenoma-carcinoma sequence" to a mass-forming ICC (peripheral small duct-type ICC) derived from BDA. Monitoring of TVDT is strongly recommended during the follow-up period of BDA. Detailed histopathological and genetic examination of the transformation of BDA to ICC is warranted.

Conflicts of Interest

All Authors have no conflicts of interest to declare in relation to this article.

Authors' Contributions

Manuscript writing: Oda E, Beppu T. Substantial contributions to conception: Yamamura K, Yuki H, Motohara T, Miyamaoto H. Technical supports and interpretation: Beppu T, Yamamura K, Hara Y, Matsumura K, Akahoshi S, Kinoshita K, Matsumura F. Histopathological diagnosis: Onishi K, Komohara Y.

Acknowledgements

Department of Community Network Pathology is supported with an unrestricted grant from the Chemo-Sero-Therapeutic Research Institute (KAKETSUKEN).

References

1 Lawrence B, Gustafsson BI, Chan A, Svejda B, Kidd M and Modlin IM: The epidemiology of gastroenteropancreatic neuroendocrine tumors. Endocrinol Metab Clin North Am *40(1)*: 1-18, vii, 2011. PMID: 21349409. DOI: 10.1016/j.ecl.2010.12.005

2 Akirov A, Larouche V, Alshehri S, Asa SL and Ezzat S: Treatment options for pancreatic neuroendocrine tumors. Cancers (Basel) *11(6)*: 828, 2019. PMID: 31207914. DOI: 10.3390/cancers11060828

3 Bartolini I, Bencini L, Risaliti M, Ringressi MN, Moraldi L and Taddei A: Current management of pancreatic neuroendocrine tumors: from demolitive surgery to observation. Gastroenterol Res Pract *2018*: 9647247, 2018. PMID: 30140282. DOI: 10.1155/2018/9647247

4 Cloyd JM, Wiseman JT and Pawlik TM: Surgical management of pancreatic neuroendocrine liver metastases. J Gastrointest Oncol *11(3)*: 590-600, 2020. PMID: 32655938. DOI: 10.21037/jgo.2019.11.02

5 Yao JC, Shah MH, Ito T, Bohas CL, Wolin EM, Van Cutsem E, Hobday TJ, Okusaka T, Capdevila J, de Vries EG, Tomassetti P, Pavel ME, Hoosen S, Haas T, Lincy J, Lebwohl D, Öberg K and RAD001 in Advanced Neuroendocrine Tumors, Third Trial (RADIANT-3) Study Group: Everolimus for advanced pancreatic neuroendocrine tumors. N Engl J Med *364(6)*: 514-523, 2011. PMID: 21306238. DOI: 10.1056/NEJMoa1009290

6 Ronot M, Cuccioli F, Dioguardi Burgio M, Vullierme MP, Hentic O, Ruszniewski P, d'Assignies G and Vilgrain V: Neuroendocrine liver metastases: Vascular patterns on triple-phase MDCT are indicative of primary tumour location. Eur J Radiol *89*: 156-162, 2017. PMID: 28267533. DOI: 10.1016/j.ejrad.2017.02.007

7 Allaire GS, Rabin L, Ishak KG and Sesterhenn IA: Bile duct adenoma. A study of 152 cases. Am J Surg Pathol *12(9)*: 708-715, 1988. PMID: 3046396. DOI: 10.1097/00000478-198809000-00007

8 Lee KB: Histopathology of a benign bile duct lesion in the liver: Morphologic mimicker or precursor of intrahepatic cholangiocarcinoma. Clin Mol Hepatol *22(3)*: 400-405, 2016. PMID: 27729636. DOI: 10.3350/cmh.2016.0105

9 Nakanuma Y, Sato Y, Ikeda H, Harada K, Kobayashi M, Sano K, Uehara T, Yamamoto M, Ariizumi S, Park YN, Choi JH and Yu E: Intrahepatic cholangiocarcinoma with predominant "ductal plate malformation" pattern: a new subtype. Am J Surg Pathol *36(11)*: 1629-1635, 2012. PMID: 23073321. DOI: 10.1097/PAS.0b013e31826e0249

10 Sasaki M, Sato Y and Nakanuma Y: Bile duct adenoma may be a precursor lesion of small duct type intrahepatic cholangiocarcinoma. Histopathology *78(2)*: 310-320, 2021. PMID: 33405289. DOI: 10.1111/his.14222

11 Kwon AY, Lee HJ, An HJ, Kang H, Heo JH and Kim G: Intrahepatic cholangiocarcinoma with ductal plate malformation-

like feature associated with bile duct adenoma. J Pathol Transl Med *49(6)*: 531-534, 2015. PMID: 26265688. DOI: 10.4132/jptm.2015.06.19

12 Tang M, Li Y, Lin Z, Shen B, Huang M, Li ZP, Li X and Feng ST: Hepatic nodules with arterial phase hyperenhancement and washout on enhanced computed tomography/magnetic resonance imaging: how to avoid pitfalls. Abdom Radiol (NY) *45(11)*: 3730-3742, 2020. PMID: 32377756. DOI: 10.1007/s00261-020-02560-0

13 An C, Park S and Choi YJ: Diffusion-weighted MRI in intrahepatic bile duct adenoma arising from the cirrhotic liver. Korean J Radiol *14(5)*: 769-775, 2013. PMID: 24043970. DOI: 10.3348/kjr.2013.14.5.769

14 Sano S, Yamamoto Y, Sugiura T, Okamura Y, Ito T, Ashida R, Ohgi K, Aramaki T, Nakanuma Y and Uesaka K: The radiological differentiation of hypervascular intrahepatic cholangiocarcinoma from hepatocellular carcinoma with a focus on the CT value on multi-phase enhanced CT. Anticancer Res *38(9)*: 5505-5512, 2018. PMID: 30194209. DOI: 10.21873/anticanres.12884

15 De Rose AM, Cucchetti A, Clemente G, Ardito F, Giovannini I, Ercolani G, Giuliante F, Pinna AD and Nuzzo G: Prognostic significance of tumor doubling time in mass-forming type cholangiocarcinoma. J Gastrointest Surg *17(4)*: 739-747, 2013. PMID: 23292461. DOI: 10.1007/s11605-012-2129-6

16 Cucchetti A, Vivarelli M, Piscaglia F, Nardo B, Montalti R, Grazi GL, Ravaioli M, La Barba G, Cavallari A, Bolondi L and Pinna AD: Tumor doubling time predicts recurrence after surgery and describes the histological pattern of hepatocellular carcinoma on cirrhosis. J Hepatol *43(2)*: 310-316, 2005. PMID: 15970351. DOI: 10.1016/j.jhep.2005.03.014

17 Cucchetti A, Russolillo N, Johnson P, Tarchi P, Ferrero A, Cucchi M, Serenari M, Ravaioli M, de Manzini N, Cescon M and Ercolani G: Impact of primary cancer features on behaviour of colorectal liver metastases and survival after hepatectomy. BJS Open *3(2)*: 186-194, 2018. PMID: 30957066. DOI: 10.1002/bjs5.100

18 Akahoshi S, Yamamura K, Sato N, Oda E, Kinoshita K, Yuki H, Motohara T, Deguchi A, Komohara Y and Beppu T: A hepatic sclerosed hemangioma with drastic changes in contrast-enhanced ultrasonography. Clin J Gastroenterol *13(6)*: 1252-1257, 2020. PMID: 32705537. DOI: 10.1007/s12328-020-01194-5

19 Aishima S, Tanaka Y, Kubo Y, Shirabe K, Maehara Y and Oda Y: Bile duct adenoma and von Meyenburg complex-like duct arising in hepatitis and cirrhosis: pathogenesis and histological characteristics. Pathol Int *64(11)*: 551-559, 2014. PMID: 25329860. DOI: 10.1111/pin.12209

20 Pujals A, Bioulac-Sage P, Castain C, Charpy C, Zafrani ES and Calderaro J: BRAF V600E mutational status in bile duct adenomas and hamartomas. Histopathology *67(4)*: 562-567, 2015. PMID: 25704541. DOI: 10.1111/his.12674

Received August 23, 2021
Revised September 2, 2021
Accepted September 3, 2021